Topics in Catalysis Vol. 38, Nos. 1–3, July 2006 (© 2006)
DOI: 10.1007/s11244-006-0074-x

Development of the ReaxFF reactive force field for mechanistic studies of catalytic selective oxidation processes on $BiMoO_x$

William A. Goddard III*, Adri van Duin, Kimberly Chenoweth, Mu-Jeng Cheng, Sanja Pudar, Jonas Oxgaard, Boris Merinov, Yun Hee Jang, and Petter Persson

Materials and Process Simulation Center (139-74), California Institute of Technology, Pasadena, CA 91125, USA

We have developed a new reactive force field, ReaxFF, for use in molecular dynamics (MD) simulations to investigate the structures and reactive dynamics of complex metal oxide catalysts. The parameters in ReaxFF are derived directly from QM and have been validated to provide reasonable accuracy for a wide variety of reactions. We report the use of ReaxFF to study the activation and conversion of propene to acrolein by various metal oxide surfaces. Using high-remperature MD-simulations on metal oxides slabs exposed to a propene gas phase we find that (1) Propene is not activated by MoO_3 but it is activated by amorphous Bi_2O_3 to form allyl which does not get oxidized by the surface; (2) Propene is activated by $Bi_2Mo_3O_{12}$ to form an allyl-radical and the hydrogen gets abstracted by a Mo=O bond, which is bridged via an O to a Bi-site; (3) Propene is activated over V_2O_5 to form an allyl, which is then selectively oxidized on the surface to form acrolein. The propene reations on V_2O_5 occur at lower temperatures than on Bi_2O_3 or $Bi_2Mo_3O_{12}$. The results are all consistent with experimental observations, encouraging us that such investigations will enhance our mechanistic understanding of catalytic hydrocarbon oxidation sufficiently to suggest modifications for improving efficiency and/or selectivity.

KEY WORDS: mixed metal oxide; bismuth molybdate; bismuth oxide; molybdenum oxide; vanadium oxide; hydrocarbon oxidation; ReaxFF; reactive force field

1. Introduction

Catalysts performing selective oxidation and ammoxidation of hydrocarbons are of major commercial importance, representing one-quarter of the value produced by catalytic processes worldwide [1]. In particular, a single catalytic process, selective ammoxidation of propylene using bismuth–molybdate and multi-metal–oxide (MMO) catalysts, accounts for the majority of the 8 billion pounds of acrolein produced annually [2]. Despite the commercial success of this process it is far from optimal and even small improvements in the catalytic efficiency can have a major impact on the energy requirements and environmental impact. In order to provide a foundation for improving this process we report here investigations of the mechanism for this process using multiscale molecular modeling techniques, and based on the mechanism to seek modifications likely to improved efficiency or selectivity.

An even larger impact would be the replacement of the relatively expensive feedstock *propene* with the more abundant and significantly cheaper *propane*. This has motivated a great deal of research by industrial chemists over the past two decades, but efficient solutions have been elusive. Breakthroughs by Mitsubishi and by BP report direct conversion from propane to acrylonitrile using very complex mixed-metal oxides (involving oxides of Mo, V, Nb, Ta, Te, plus alkali and other metals for which there may be several stable phases), hereafter denoted as MMO [3]. Although the ability of these MMO catalysts to convert propane directly to acrylonitrile ($H_2C=CH–CN$) and/or acrolein ($H_2C=CH–HC=O$) is impressive, the selectively and reactivity are not yet adequate for industrial use.

To optimize these catalysts, we believe that it is essential to determine the chemical mechanisms underlying the catalysts and to predict how the processes can be changed to improve selectively and activity. However the enormous complexity of the MMO catalysts has made it difficult to extract from experimental data sufficient information about the mechanism. These catalysts have very complex structures with perhaps 100's of atoms per cell with perhaps several distinct catalytic sites, which is additionally complicated by reconstruction and non-stoichiometry at the surface. The resulting general lack of knowledge regarding the role of the various metals in the MMO catalysts has hindered progress in improving these catalysts, which has been empirical and too slow [4].

Our approach is to use first principles methods to determine the mechanisms for these processes and to use these mechanisms to design modifications likely to improve efficiency and/or selectivity. Unfortunately it is not practical to use accurate QM to describe the large disordered and reconstructed cells of the MMO catalysts while simulating the processes of formation, activation,

* To whom correspondence should be addressed.
E-mail: wag@wag.caltech.edu

and reactions for the various compositions and methods of preparation that generally result in very complex and poorly characterized structures.

To provide a practical alternative to QM-simulations of the chemistry on such complex systems we have developed the ReaxFF strategy for reactive force fields that can be used in large scale MD calculations while describing accurately the activation barriers and reaction mechanisms of complex chemical reactions. The parameters for ReaxFF are derived entirely from QM without the use of empirical data, making it applicable to novel systems on which there is little or no experimental data. ReaxFF based MD-simulations allow us to examine the reactions under conditions of high temperature and pressure used experimentally.

We report here key elements in the development of the ReaxFF for V_xO_y, Bi_xO_y, Mo_xO_y, and $Bi_xMo_yO_z$ systems and results from high-temperature ReaxFF MD-simulations on propene reactions at the surface of these metal oxide materials.

2. Methodology

Because of the extreme complexity and the dearth of mechanistic experimental data regarding the selective oxidation of current propane over MMO catalysts, we believe that first principles computational techniques provide the only effective means to make progress. However, this system is complex and may require accurate energy surfaces for reactions involving many 1000s of atoms. The computational expense of QM-calculations restricts these methods to small systems and short time-scales, making them mainly applicable to the characterization of idealized chemical processes, involving simple, ordered structures at zero temperature. These limitations make it virtually impossible to use *only* QM-methods in obtaining a full understanding of the intricate reaction paths of a system as complex as a MMO catalyst, as it is essential to have a fast computational method that can identify the critical configurations, including high-energy intermediates and transition states. However, our recent advances in ReaxFF present realistic possibilities of successfully carrying out this process.

2.1. ReaxFF reactive force fields

2.1.1. Overview

Over the last 5 years we have been developing the first principles-based ReaxFF reactive force fields and have now demonstrated that ReaxFF is capable of reproducing the energy surfaces, structures, and barriers from accurate QM-calculations for reactive systems. ReaxFF studies have been reported for a wide range of materials, including hydrocarbons [5], nitramines [6], ceramics [7] (Si/SiO_2), metals and metal oxides [8], metal/hydrocarbon interactions [9] and metal hydrides [10] demonstrating that ReaxFF has the versatility required to capture the complexity of the mixed metal catalyst system.

ReaxFF includes the following features:

- *Environmentally dependent charge distributions on atoms*. In ReaxFF the Coulomb interaction between two atoms is shielded for small distances so that it can include the electrostatic interactions between bonded atoms (not excluded as common with normal FF). The total magnitude of the charge on each atom is allowed to change depending on the environment. Thus an H next to C is generally positive while a C next to an O is generally positive. The ReaxFF charge parameters, which consist of electronegativity, hardness, and shielding parameter for each element, are optimized to reproduce QM-derived charge distributions. The exact amount of the charge transfer depends on the nature of the atoms and the distances between them, allowing the atom charge distributions to change during reactions to describe the effects of changes in charge distribution on conformational and reactive events [11].
- *Bond order dependent valence terms*. All valence terms (bonds, angles, and torsions) depend on the bond order, providing a smooth description of chemical reactions. The bond orders are determined uniquely from the interatomic distances allowing ReaxFF to recognize and handle the changes in connectivity during reactions. All parameters describing the valence terms are derived directly from QM studies on a large number (1000's) of reactions (allowed and forbidden) and are universal.
- *Non-bond or van der Waals interactions*. Most critical in a FF is to properly account for the short range repulsion and steric interactions arising directly from the Pauli principle. To provide the data for this, we obtain the equation of state from QM for bulk phases involving a variety of coordinations. Thus for metals we typically include coordinations of 12 (fcc and hcp), 8 (bcc), 6 (simple cubic), 4 (diamond), and mixed (A15). We use a Morse function (three parameters) to describe the short range repulsion and to include long range attraction. These non-bonding interactions are included between *every* atom pair, independent of connectivity. Excessive short-range attractions or repulsions are avoided by including a shielding term in the non-bond potentials.

Furthermore, the following guiding principles were adopted during the development of the ReaxFF reactive potentials:

- *No discontinuities in energy or forces*. Even during reactions, ReaxFF provides a continuous energy and force description, thus allowing proper reactive MD-simulations.

- *Transferable potential*. Each element is described by just one atom type, allowing good transferability of the force field to new systems and avoiding complicated atom type modification during reactions.
- *No predefinition of reactive sites*. With ReaxFF, one does not need to predefine where and when they expect reactions to occur. We typically heat a gas of molecules near a surface and allow the reactions to proceed, allowing unbiased simulations on reactive systems.

2.2. QM-methods

In order to parameterize ReaxFF we performed a number of periodic and non-periodic QM-calculations. The non-periodic QM-calculations were performed using the B3LYP [12] hybrid DFT function as implemented in the Jaguar 5.0 program package (Schrödinger Inc. Portland, Oregon 2000). For the V, Mo, and Bi metals we used the LACVP** Hay and Wadt [13] core-valence (relativistic) effective core potential to treat the outer core and valence electrons explicitly (thus for Mo we include the 6 valence electrons plus the eight 3s and 3p core electrons for a total of 14 electrons). This uses the valence double-ζ contraction of the optimized atomic basis set sets. For the C, O, and H atoms all electrons were treated explicitly using the Pople 6-31G** basis set [14]. The Periodic QM-calculations were performed using the SeqQuest program [15]. This uses the PBE GGA exchange-correlation functional. The Gaussian basis sets were optimized at the core-valence double-ζ contraction level.

All QM-calculations were performed for all plausible spin states. For open-shell systems, QM-calculations were performed using the spin-unrestricted DFT (UDFT). ReaxFF does not include the concept of multiple spin states and is parameterized to reproduce the energy corresponding to the lowest energy spin state.

2.3. Molecular dynamics simulations

To evaluate the steps involved in catalytic hydrocarbon oxidation over MMO, we generated a metal oxide slab of about 500 atoms and exposed this on both sides to a gas phase containing 20 propene molecules. This system was energy minimized and equilibrated at 500 K with the ReaxFF program. Subsequently, a dual-temperature simulation was performed, in which the metal oxide slab was kept at $T = 500$ K while the hydrocarbon phase was gradually heated (at a rate of 0.016 K/fs) from 500 K to 2500 K during a 125 ps NVT/MD-simulation. The temperature was controlled using a Berendsen thermostat with a temperature damping constant of 0.1 ps. A MD-timestep of 0.25 fs was used in these simulations.

3. Review of the known chemistry

The goal of this research is to provide the level of understanding required to develop new generation catalysts for selective oxidation and ammoxidation of propane and other alkanes. There are many questions about the structures and fundamental steps of the catalytic processes that we must investigate: The first step is to see how well ReaxFF MD reproduces the known observations from experiment.

Here we will focus on the simpler case of the direct conversion of propene to acrolein. This is still quite complex, with removal of two hydrogens to form H_2O and adding the O from O_2 in a series of steps. Plausible steps in the mechanism include:

- CH activation of propene to form allyl.
- Interaction of allyl with a M = O bond form a bonded Mo–O–CH_2–CH = CH_2 species.
- An additional hydrogen extraction to form and desorb acrolein, O = CH–CH = CH_2.
- Re-oxidation of the surface by molecular O_2 to form species, such as bulk [O^{2-}] that may diffuse to the reaction site.
- Reaction of the H's removed from the substrate by M = O bonds to form M–OH and eventually reacting to desorb H_2O.We report here an examination of the oxidation of propene by $BiMoO_x$ catalysts, where we can compare to a large body of experimental evidence.

3.1. Surface structure of MMO

There is evidence that the favorable crystal structure for activating alkanes involves an intimate mixture of Mo oxidation states. Thus the ethane dehydrogenation catalyst developed by Union Carbide was based on the Mo_5O_{14} structure, which has three Mo^{VI} sites and two Mo^{V} sites. The optimum catalyst here had the composition $Mo_{0.61-0.77}V_{0.31-0.19}Nb_{0.08-0.04}$ and the recent re-optimization of this catalyst by Symyx lead to a composition of $Mo_{73}V_{24}Nb_3$ [16]. Similarly the MMO catalyst also involves an intimate interplay between various oxidation states of the multiple metals comprising the active site but also between multiple phases. The structures of the three crystalline phases comprising the Mo–V–Nb–Te–O catalyst were recently solved and include the orthorhombic M1 phase ($Mo_{7.8}V_{1.2}NbTe_{0.94}O_{28.9}$), the pseudo-hexagonal M2 phase ($Mo_{4.67}V_{1.33}Te_{1.82}O_{19.82}$), and a trace amount of the monoclinic $TeMo_5O_{16}$ phase [17]. The M1 phase is generally accepted as the primary phase responsible for activating propane, most likely converting it to propene. The M2 phase does not activate propane but can selectively convert propene to acrylonitrile. There is also a little understood synergistic effect observed between the phases but it

has been shown that the beneficial effect of the M2 phase is not observed for physical mixtures with grains larger than 250 μm indicating that the phase cooperation effect is occurring on a nanoscale [18].

The M1 phase forms rod-like crystals and upon grinding results in higher conversion rates indicating that the [001] surface contains the active site [19]. Compared with the bulk crystal, the surface contains a slightly lower concentration of V and a slightly higher concentration of both Nb and Te. [20] It has been proposed that Nb occupies the same crystallographic sites as V and it may also stabilize Te at the surface. However, preparation of the MMO catalysts is very challenging and can be affected by many factors including the method of preparation as well as the calcination treatment resulting in difficulty with reproducibility. Slight variations in the fractional occupancies of the metals does not alter the structure of the catalyst but can change the activity/selectivity of the catalyst [21]. By using computational methods, we can explore in detail how variations in the surface alter the performance of the catalyst as well as the function of each metal.

We believe that determining and describing the possible surface configurations, active sites, and the occlusion of these sites by the various metals is critical to this project. Thus we will spend considerable effort in developing the ReaxFF to provide good structures and energetics and in using the ReaxFF in MD and MC simulations to determine the distribution of stable surface configurations under various conditions. These studies will be aimed at understanding the structures and active configurations at the reaction temperatures. We anticipate that there will be some unusual structures that may have unusual chemistries. This will lead to QM-calculations to validate the predictions from ReaxFF and to continually improve the force field.

3.2. Mechanism for selective oxidation and ammoxidation of propene by $BiMoO_x$ catalysts

Our previous research on the mechanism for selective oxidation and ammoxidation of propene used only QM on small models of the bismuth–molybdate catalysts [22,23]. Figure 1 summarizes the mechanism for selective oxidation of propene to acrolein while figure 2 summarizes the functionalization step of the selective ammoxidation of propene to acrylonitrile. This mechanism explains the kinetics observed for the ammoxidation process. Thus Grasselli and coworkers found that at low partial pressures of feed ($pC_3H_6 = 0.041$ atm), the product ratio is a linear function of the NH_3/C_3H_6 ratio (indicating that one ammonia molecule is involved at the N-insertion site per catalytic cycle) whereas at intermediate and high partial pressures of feed ($pC_3H_6 = 0.082$ atm and 0.14 atm) the product ratio is a linear function of $(NH_3)^2/C_3H_6$, corresponding to two ammonia molecules activated at the N-insertion site per acrylonitrile. Thus, with one exception, these mechanisms are now accepted by the experimental community [24].

The exception in the agreement between theory and experiment is that the QM-calculations suggests that only Bi^V centers can activate the allylic H bond of propene required in the first step of this process. In contrast the experimentalists believe that Bi^{III} centers are involved. This is because bulk Bi_2O_3 is observed to activate a small amount of propene to hexadiene, but without oxidation. We have speculated that bulk Bi_2O_3 may have Bi^V sites at the surface (or perhaps some other activated site that can do the chemistry) under reaction conditions. With $BiMoO_x$, there are increased possibilities for Bi^V centers. However the current ReaxFF simulations described below show that a surface in which all Bi have the form of Bi^{III} can activate propene to form allyl. As discussed below this activation is at Mo=O bonds, but for sites in which the Mo is connected to a Bi through an O bridge.

We have now reexamined some steps in the mechanism of selective oxidation of propene to acrolein over $BiMoO_x$, using ReaxFF described to describe realistic surfaces at realistic reaction temperatures. Here we will consider both the activation and functionalization processes.

This required extending the ReaxFF to handle Bi oxides (Bi^{III} and Bi^V) and the various $BiMoO_x$ mixed oxides. Our goal here is a relatively complete characterization of these systems under realistic conditions. This will set the stage for the much more challenging case of the propane ammoxidation process.

3.3. Mechanisms for selective oxidation and ammoxidation of propane by $MoVNbTaTeO_x$ (MMO) catalysts

3.3.1. Activation

The generally accepted first step in the process is *oxydehydrogenation of the propene* to form the allyl radical (figure 3) which is analogous to the propene oxidation mechanism in the bismuth molybdate catalyst. Currently the best oxydehydrogenation catalysts are vanadia (V_2O_5) based, which might explain the presence of V in existing propane catalysts.

There is also substantial experimental evidence that existing industrial propane oxidation or ammoxidation processes exhibits a propylene intermediate with a measurable lifetime [25]. This could indicate that a main cause for the lower activity of propane might be hydrogen saturation of the surface. Thus it is not clear whether *more* dehydrogenation sites are required or whether *different* dehydrogenation sites are required.

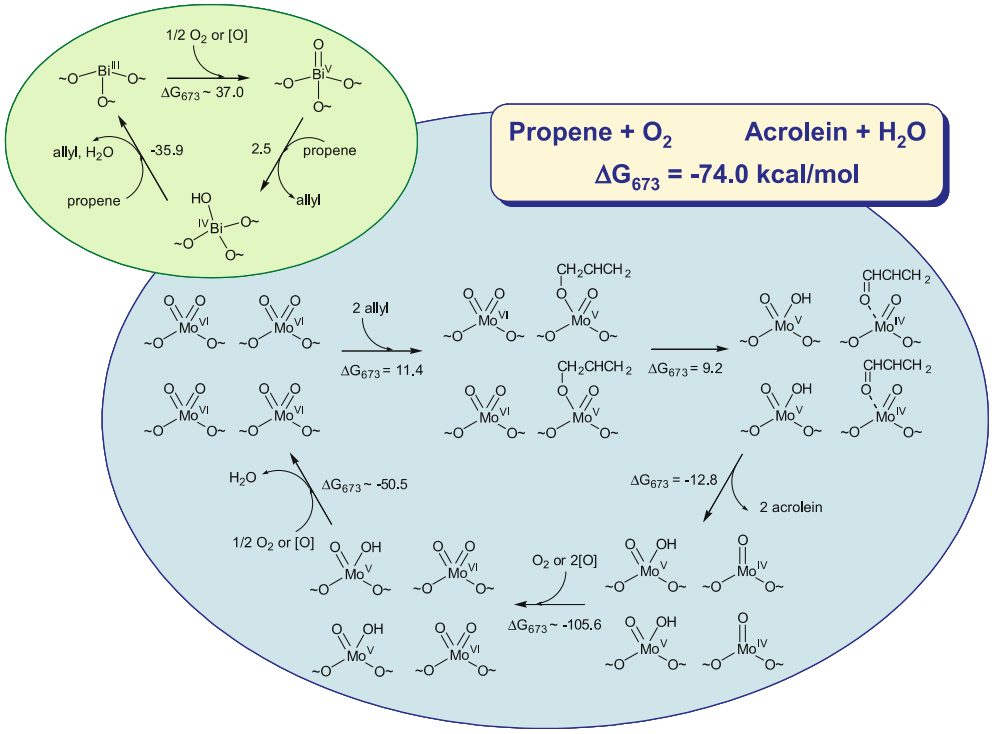

Figure 1. The dual-oxo mechanism for selective oxidation of propene by $BiMoO_x$ [22,23].

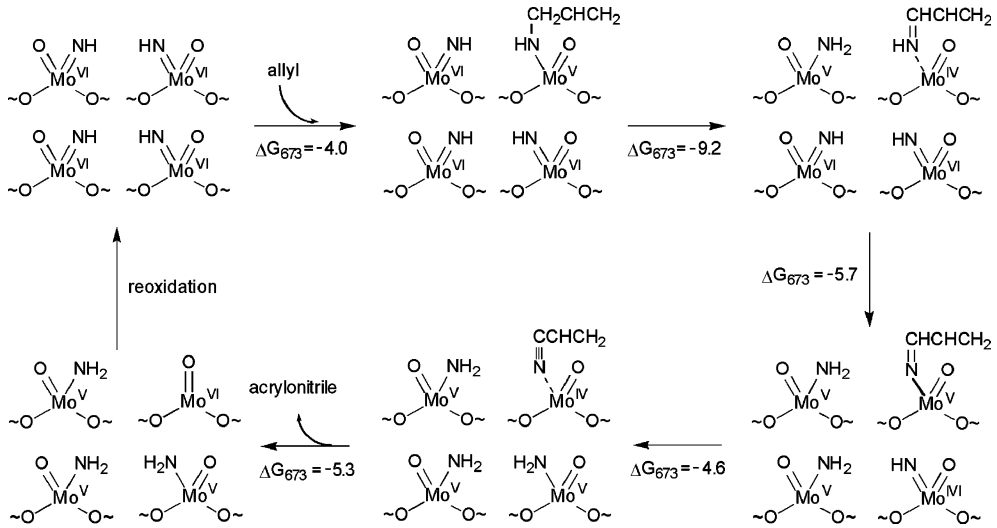

Figure 2. The four-site mechanism for ammoxidation of propene by BiMoO*x* [22,23].

For $BiMoO_x$ designing more dehydrogenation sites might increase the Bi/Mo ratio above the value found optimal for propene chemistry. Since Bi is essential for activating the first CH bond of propene in the $BiMoO_x$ catalyst, one can speculate that in MMO, it might be a Te site or perhaps Te associated with V or another metal that is responsible for activating the first CH bond of propane. Indeed it might be the V is important since experiments show that supported vanadia is the most active and selective simple metal oxide for alkane oxidative dehydrogenation, possibly because its reducible nature leads to the rapid redox cycles required for a catalytic turnover [26]. We also anticipate that there might be Te substitutions on Mo sites over-coordinated with oxygen atoms that become more willing to accept hydrogen, losing metal–oxygen bonds to relieve the over-coordination. It is also potentially possible that such extra hydrogens can be intercepted by molecular oxygen, catalyzed by such known oxygen activators as Pd or Pt.

All these possibilities, as well as the initial step, can be explored by the combined ReaxFF/QM methodology

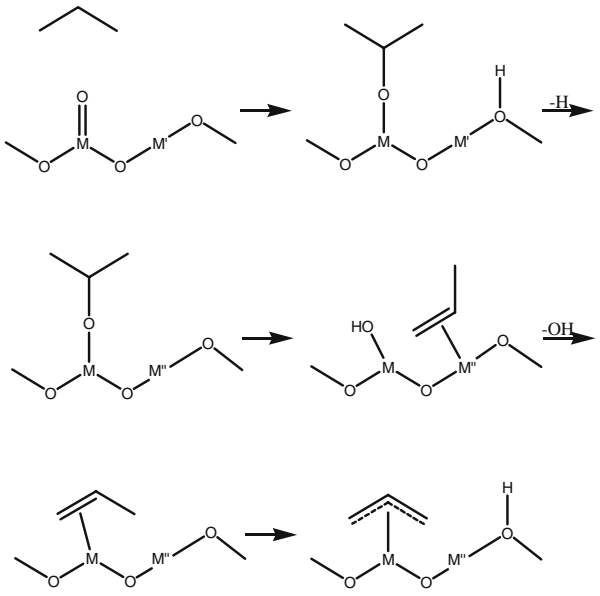

Figure 3. Proposed mechanism for the oxydehydrogenation of propane.

described above. ReaxFF, trained against a wide range of QM-data, will allow us to rapidly screen the catalytic potential of various metal/metal oxide surface sites at realistic sample sizes, temperatures and substrate pressures, thus identifying the critical reactions and surface configurations Once these critical events are identified and confirmed by QM-simulations we aim to use this information to improve catalyst design.

The propylene intermediate is subsequently oxydehydrogenated as well. This step is probably quite similar to the oxydehydrogenation step in the propylene process, but now it might occur at either a Mo site or at a V site. Investigation of this step is expected to be quite similar to the preceding step, although complicated by the possibility of inhibition.

Other questions we propose to investigate are: Is this a sequential process, followed by dissociation and migration of propylene, or can all three dehydrogenations be achieved in succession at the same site? Does each dehydrogenation occur on different oxygen atoms, or can multiple ones occur on the same atom? What effect do the different metals have on the first and the second steps?

4. Results

4.1. Force field development

4.1.1. General

To define the ReaxFF parameters we performed QM-simulations on a range of small metal oxide clusters, covering various metal oxidation states. These clusters were first minimized and subsequently distorted by dissociating specific bonds or by bending specific valence angles. The QM-energy differences between the undistorted and distorted systems were subsequently used to train the ReaxFF parameters. Furthermore, we also calculated Mulliken charges for these metal oxide clusters and used these to derive the ReaxFF electronegativity, hardness, and shielding parameters. To ensure that ReaxFF would not artificially favor non-physical high metal oxidation states we also performed QM-simulations on small, high-oxidation state clusters (e.g. MoO_4) and tested ReaxFF against their QM-derived heats of formation. A detailed comparison of these QM and ReaxFF will be reported in papers to be published elsewhere.

4.1.2. Metal oxide bulk phases

To enable ReaxFF to describe oxidation reactions on metal oxide surfaces we developed a QM-based training set for condensed phase Mo_xO_y, Bi_xO_y, and V_xO_y systems and for metallic Mo, Bi and V-phases. This training set considered both the stable oxidation states and also contained information on over-oxidized and under-oxidized metal oxide systems. Figure 4 shows the ReaxFF and QM-derived heats of formations for these metal oxide phases, demonstrating that ReaxFF is capable of describing multiple metal oxidation states. ReaxFF has a systematic tendency to overestimate the stability of the metal oxide phases, but the energy differences for oxidation changes (i.e. V_2O_5 to V_2O_3) are in good agreement with the QM-data, indicating that ReaxFF is able to capture the energetics of redox-reactions at metal oxide surfaces.

4.1.3. Reactivity between hydrocarbons and small Mo_xO_y, Bi_xO_y, and V_xO_y-clusters

We have compared the QM and ReaxFF energies for various substrates, products, and intermediates involved in the conversion of propene to acrolein and in related hydrocarbon oxidation reactions, catalyzed by Mo_3O_9, Bi_xO_y, and V_4O_{10}-clusters. We found good agreement between QM and ReaxFF for all these reactions, which involve 1- and 2-fold reduction of the metallic sites. Figures 5, 6, 7 show ReaxFF and QM-results for some key reactions involved in catalytic oxidation of hydrocarbons.

4.2. Low-temperature ReaxFF simulations on the reaction barriers for propene to acrolein conversion on metal oxide slabs

After parameterizing ReaxFF against the data described in the previous sections we determined the ReaxFF reaction profile for propene to acrolein conversion on the 001 surface of V_2O_5, the 010 surface of MoO_3, and the 010 surface of α-Bi_2O_3 using a low-temperature (50 K) MD/NVT-simulation with shifting bond restraints to drive the reaction coordinate. Figures 8, 9, 10 show the results from these simulations.

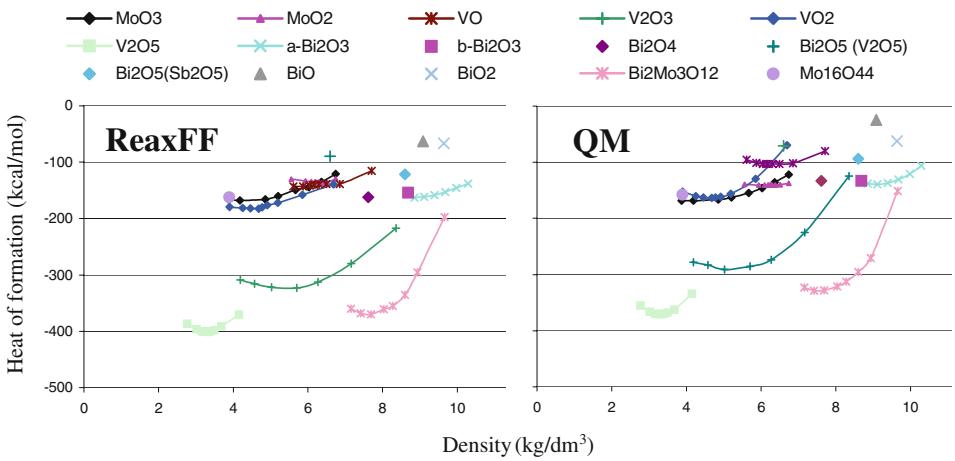

Figure 4. Heats of formation and energy/density relations for various Mo, V, and Bi-oxides from ReaxFF and QM.

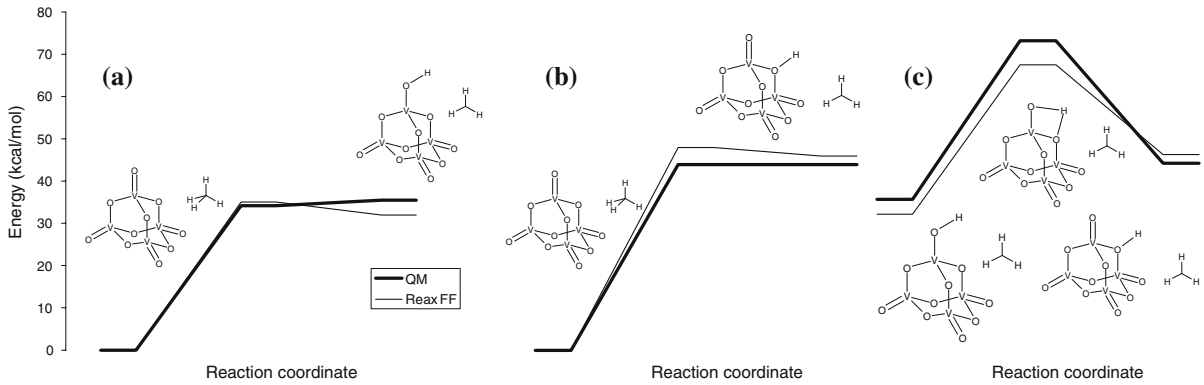

Figure 5. Reaction energetics from QM and ReaxFF calculations. (a, b) hydrogenation of a V_4O_{10}-cluster by methane (c) hydrogen shift between a terminal and a bridging –OH-group.

We find that the MoO_3-slab has the highest barrier for the first hydrogen abstraction step (34 kcal/mol), while this barrier is the lowest on Bi_2O_3 (22 kcal/mol).

On the Bi_2O_3-slab, however, we find a substantial barrier for allyl binding to the surface (~15 kcal/mol). This barrier is negligible on both MoO_3 and V_2O_5. This indicates that while Bi_2O_3 can generate allyl radicals, these radicals may not bind to the surface to get oxidized. This is consistent with experimental findings that propene exposure to bismuth oxide surfaces result primarily in formation of hexadiene, not in the formation of oxidized hydrocarbons [27].

On the V_2O_5 surfaces we find that oxidation should dominate dimerization, since no substantial barriers remain after the first dehydrogenation step. Pure vanadium pentoxide is known to be active for oxidation of hydrocarbons though the selectivity to partial oxidation products is poor [28]. The high barrier observed for MoO_3 is consistent with the observed inactivity of MoO_3 for allylic oxidation of propene [29]. We note that the propene to acrolein conversion is exothermic on the MoO_3-slab by about 20 kcal/mol (figure 9), while it is endothermic by about 50 kcal/mol on the Mo_3O_9-cluster (figure 6). This is probably related to the low-oxidation state Mo-atoms formed by the dehydrogenation and oxidation steps compensating for their reduction by strengthening their remaining Mo–O bonds in the MoO_3-slab, a process likely to be far less effective in the small Mo_3O_9-cluster. This probably corresponds to the spectator oxo stabilization discovered in earlier studies on these systems [22,23,30–36].

4.3. *High-temperature ReaxFF MD-simulations*

In figures 8–10 we imposed a reaction coordinate during low-temperature MD-simulations to determine reactions barriers. In order to provide unbiased information on the catalytic conversion of propene on metal oxide slabs, we then performed high-temperature, unrestrained MD-simulations. The initial hydrogen abstraction barrier (>20 kcal/mol) is such that MD-simulations at normal catalysis temperatures ~650 K may take 1 ns to 1 μs. Thus for proof-of-concept studies to be reported here, we increased the system temperature to observe the activation and subsequent oxidations more quickly. This leads to indications of relative

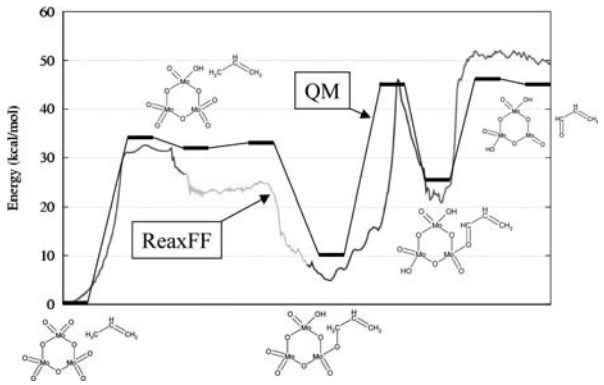

Figure 6. Reaction profile from QM and ReaxFF calculations for the conversion of propene to acrolein on a Mo_3O_9-cluster. ReaxFF results were obtained by a low-temperature (50 K) MD-simulation employing shifting bond restraints to drive the reaction coordinate and were performed on a single Mo_3O_9-cluster and propene molecule (as depicted in this figure); QM simulations were performed with "fresh" Mo_3O_9-clusters for each reaction step (dehydrogenation, allyl adsorption, 2nd dehydrogenation, acrolein desorption).

conversion rates and suggestions for active catalytic sites. These active sites can subsequently be studied at low-temperatures and by QM-methods to validate the ReaxFF predictions.

To evaluate the validity of this ReaxFF approach we performed 125 ps simulations on a propene gas-phase, consisting of 20 propene molecules in contact with V_2O_5, Bi_2O_3, $Bi_2Mo_3O_{12}$ (010 surface), and MoO_3-slabs. The slabs were kept at 500 K during these simulations, while the propene molecules were gradually heated from 500 K to 2500 K. Figure 11 shows the molecular composition as a function of temperature, as observed from the V_2O_5/propene simulations. We find that around $T = 1600$ K propene gets converted to allyl radicals by

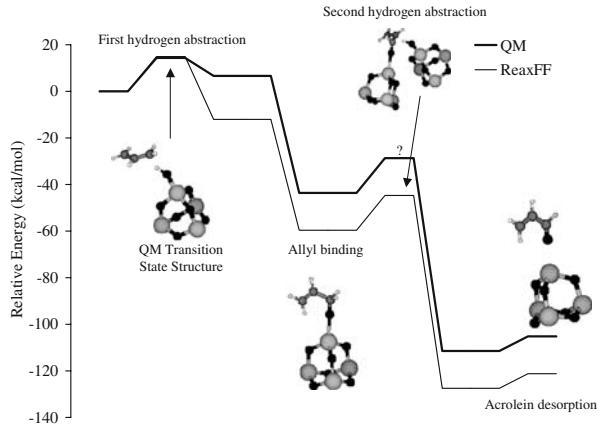

Figure 7. Reaction profile from QM and ReaxFF calculations for conversion of propene to acrolein over a Bi_4O_7-cluster. The first hydrogen abstraction, allyl binding and acrolein desorption steps were performed using a single Bi_4O_7-cluster while the second hydrogen abstraction step was performed using two clusters (as depicted). We have not yet obtained a QM transition state for the second hydrogen abstraction step.

hydrogenation of a V=O surface bond. These allyl radicals get oxidized, leading eventually to acrolein.

In the MoO_3/propene simulation no metal–oxide assisted propene conversion was observed during the course of the simulation, in accordance with the high barrier for the first hydrogen abstraction on MoO_3 (Figure 9).

On the Bi_2O_3-surface we also did not find any surface-assisted propene conversion, which was unexpected given the relatively low barrier for the initial hydrogen abstraction. We did, however, observe hydrogen abstraction on the amorphous Bi_2O_3-surface generated by heating the Bi_2O_3 slab along with the hydrocarbon phase; this propene dehydrogenation was not followed by oxidation, in agreement with experimental observations.

On the $Bi_2Mo_3O_{12}$-surface (figure 12) we observed hydrogen abstraction followed by water formation. The hydrogen abstraction resulted in the hydrogenation of a Mo=O surface bond, indicating that these bonds are easier to hydrogenate in $Bi_2Mo_3O_{12}$ compared to MoO_3. In response to the hydrogenation, this Mo significantly decreased the Mo–O bonds shared with neighboring Bi-atoms, indicating that the presence of relatively weak Bi–O bonds may be responsible for the activation of the surface Mo=O bonds in $Bi_2Mo_3O_{12}$. All hydrogen abstractions observed below 2000 K on the V_2O_5 and $Bi_2Mo_3O_{12}$ surfaces resulted in allyl radical formation, indicating that these surfaces are selective.

These simulations give a good initial indication of the relative activity of the metal oxide surfaces. Of course given the time scale of the hydrogen abstraction events at normal operation temperature, we must perform longer simulations to properly sample the surface reactivity and to identify active surface sites.

4.4. Future work

These results indicate that investigations using ReaxFF, parameterized by an extensive QM-derived training set covering all valid oxidation states and key reaction profiles, can enhance our mechanistic understanding of catalytic processes. We believe that this will allow us to identify the active catalytic sites in the complex MMO materials and to suggest modifications likely to improve efficiency and/or selectivity. We are in the process of performing more extensive simulations for a wide variety of conditions and structures to further validate the ReaxFF approach and to expand the ReaxFF methodology to MMO catalysts for ammoxidation of propane and to other metal oxides.

5. Summary

The MMO catalysts that successfully ammoxidize propane have very complex structures with 100's of

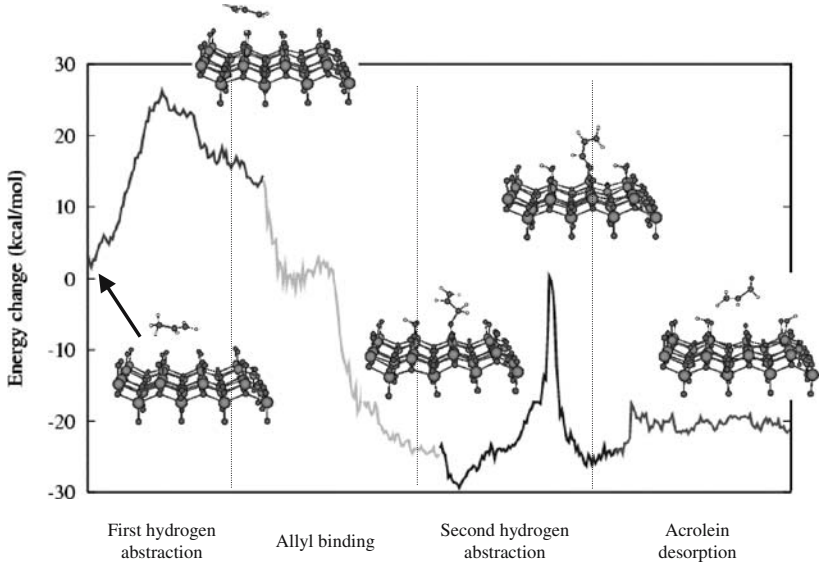

Figure 8. ReaxFF reaction profile for propene to acrolein conversion catalyzed by a V_2O_5-slab.

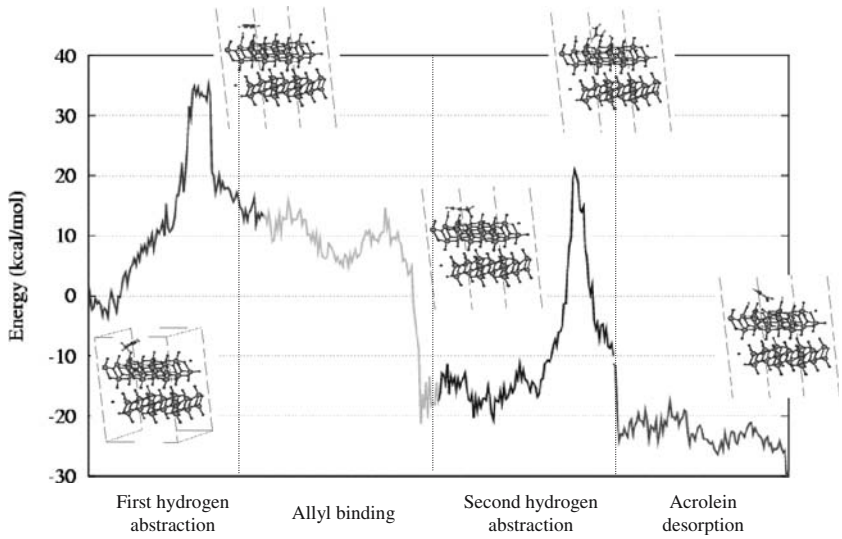

Figure 9. ReaxFF reaction profile for propene to acrolein conversion catalyzed by a MoO_3-slab.

atoms per cell, which is additionally complicated by reconstruction and non-stoichiometry at the surface. The metals used are normally Mo, Bi, V, Nb, Ta, Te, with minor amounts of other metals, further increasing the complexity. As a result, it has been difficult to use first principles theory to study such processes.

To make progress in applying theory and computation to such systems we developed the ReaxFF reactive force field suitable for MD calculations to predict the structures of these complex oxides, both under equilibrium conditions (at the temperatures and pressures of interest) and dynamically as the reactions proceed. The parameters in ReaxFF are derived directly from QM and we have demonstrated that ReaxFF gives reasonable accuracy for the reactions studied.

We then employed ReaxFF to study the high-temperature conversion of propene on various metal oxides surfaces (Bi_2O_3, MoO_3, V_2O_5, and $Bi_2Mo_3O_{12}$) and found that the ReaxFF results are in good agreement with experimental observations: V_2O_5 is the most active catalyst, Bi_2O_3, and $Bi_2Mo_3O_{12}$ are less active but can abstract hydrogens from propene while no activity was observed for MoO_3.

Our future studies will focus on elucidating the reaction mechanisms for current propene and propane ammoxidation catalysts, to identify new compositions for these catalysts expected to exhibit higher rates and selectivities, and to optimize the new catalysts with computational simulations at realistic reaction conditions.

Figure 10. ReaxFF reaction profile for propene to acrolein conversion catalyzed by a Bi_2O_3-slab.

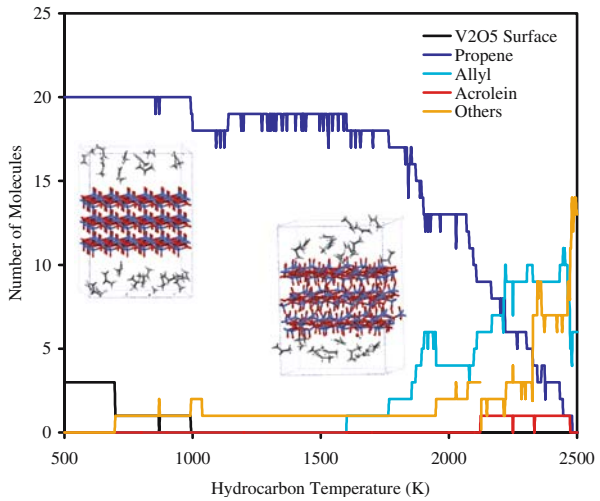

Figure 11. System composition as a function of hydrocarbon temperature as observed during the V_2O_5/propene ReaxFF MD-simulation.

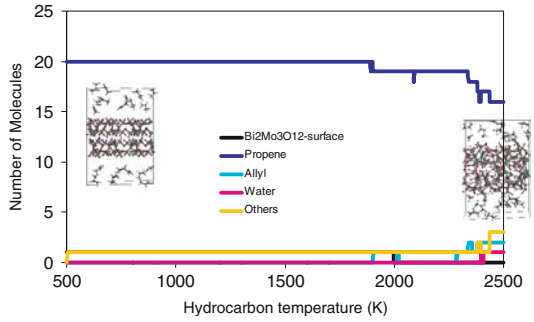

Figure 12. System composition as a function of hydrocarbon temperature as observed during the $Bi_2Mo_3O_{12}$/propene ReaxFF MD-simulation.

Acknowledgements

We thank NSF (MED ITR DMR-0427177, NANO CCF-0524490), DOE (DE-FG01-04ER04-20, DE-PS36-03GO93015), and ONR-MURI N00014-02-1-0665, N00014-05-1-0778) for partial support of the personnel working on this project and ARO-DURIP and ONR-DURIP for providing the computational resources.

References

[1] R.K. Grasselli, Catal. Today 49 (1999) 141.
[2] R.K. Grasselli, J. Chem. Ed. 63 (1986) 216.
[3] T. Ushikubo, et al., *Process for Producing Nitriles* Mitsubishi Kasei Corporation (1994) US Patent # 5,281,745.
[4] S. Bergh, P. Cong, B. Ehnebuske, S. Guan, A. Hagemeyer, H. Lin, Y. Liu, G.G. Lugmair, H.W. Turner, A. Volpe, Jr., W.H. Weinberg, L. Woo and J. Zysk, Topics Catal 23 (2003) 65.
[5] A.C.T. Duin, S. Dasgupta, F. Lorant and W.A. Goddard III, J. Phys. Chem. A 105 (2001) 9396.
[6] A. Strachan, A.C.T. Duin, S. Dasgupta, D. Chakraborty, W.A. Goddard and III, Phys. Rev. Lett. 91 (2003) 098301.
[7] A.C.T. Duin, A. Strachan, S. Stewman, Q. Zhang, W.A. Goddard and III, J. Phys. Chem. A 107 (2003) 3803.
[8] K.D. Nielson, A.C.T. Duin, J. Oxgaard, W. Deng, W.A. Goddard and III, J. Phys. Chem. A 109 (2005) 493.
[9] Q. Zhang, T. Cagin, A.C.T. Duin, W.A. Goddard and III, Phys. Rev. B 69 (2004) 045423.
[10] S. Cheung, W. Deng, A.C.T. Duin, W.A. Goddard and III, J. Phys. Chem. A 109 (2005) 851.
[11] A.K. Rappé, W.A. Goddard and III, J. Phys. Chem. 95 (1991) 3358.
[12] A.D. Becke, J. Chem. Phys. 98 (1993) 5648; C. Lee, W. Yang and R.G. Parr, Phys. Rev. B 37 (1998) 785.
[13] P.J. Hay, W.R. Wadt J. Chem. Phys. 82 (1985) 299; W.A. Goddard III, Phys. Rev. 174 (1968) 659; C.F. Melius, B.O. Olafson and W.A. Goddard III, Chem. Phys. Lett. 28 (1974) 457.
[14] P.C. Hariharan and J.A. Pople, Chem. Phys. Lett. 16 (1972) 217; M.M. Francl, W.J. Pietro, W.J. Hehre, J.S. Binkley, M.S. Gordon, D.J. DeFrees and J.A. Pople, J. Chem. Phys. 77 (1982) 3654.
[15] C. Verdozzi, P.A. Schultz, R. Wu, A.H. Edwards and N Kioussis, Phys. Rev. B 66 (2002) 125408.

[16] Y. Liu, P. Cong, R. Doolen, S. Guan, D.M. Poojary, H.W. Turner and W.H. Weinberg, 4th Eur. Congr. on Catalysis, Rimini, Italy (1999).
[17] P. Desanto, Jr., D.J. Buttrey, R.K. Grasselli, C.G. Lugmair, A.F. Volpe, Jr., B.H. Toby and T Vogt, Z. Kristallogr. 219 (2004) 152.
[18] J. Holmberg, R.K. Grasselli and A Andersson, Appl. Catal. A 270 (2004) 121.
[19] P. DeSanto Jr., D.J. Buttrey, R.K. Grasselli, C.G. Lugmair, A.F. Volpe, B.H. Toby and T Vogt, Topics Catal 23 (2003) 23.
[20] D. Vitry, Y. Morikawa, J.L. Dubois and W. Ueda, Appl. Catal. A 215 (2003) 411.
[21] R.K. Grasselli, D.J. Buttrey, P. DeSanto, Jr., J.D. Burrington, C.G. Lugmair, A.F. Volpe, Jr. and T. Weingand, Catal. Today 91–92 (2004) 251.
[22] Y.H. Jang and W.A. Goddard III, Topics Catal 15 (2001) 273.
[23] Y.H. Jang and W.A. Goddard III, J. Phys. Chem. B 106 (2002) 5997.
[24] R.K. Grasselli, J.D. Burrington, D.J. Buttrey, P. DeSanto, C.G. Lugmair, A.F. Volpe and T. Weingand, Topics Catal 23 (2003) 5.
[25] A. Hinz and A. Andersson, Chem. Eng. Sci. 54 (1999) 4407.
[26] M.D. Argyle, K. Chen, A.T. Bell and E. Iglesia, J. Catal. 208 (2002) 139.
[27] H.E. Swift, J.E. Bozik and J.A. Ondrey, J. Catal. 21 (1971) 212; W. Martir and J.H. Lunsford, J. Am. Chem. Soc. 103 (1981) 3728.
[28] B. Grzybowska-Swierkosz, Appl. Catal. A 157 (1997) 409.
[29] B. Grzybowska, J. Haber and J. Janas, J. Catal. 49 (1977) 150.
[30] J.N. Allison and W.A. Goddard III, in: *ACS Symposium Series No. 279, Solid State Chemistry lysis*, eds. R.K. Grasselli and J.F. Brazdil (American Chemical Society,Washington, DC, 1985) pp. 23-36.
[31] J.N. Allison and W.A. Goddard III, J. Catal. 92 (1985) 127.
[32] W.A. Goddard III, J.J. Low, B.D. Olafson, A. Redondo, Y. Zeiri, M.L. Steigerwald, E.A. Carter, J.N. Allison and R. Chang, in: *Proceedings of the Symposium on The Chemistry and Physics of Electro-catalysis*, Vol. 84–12, eds. J.D.E. McIntyre, M.J. Weaver and E.B. Yeager (The Electrochemical Soc., Inc., Pennington, NJ, 1984) pp. 63–95.
[33] A.K. Rappé and W.A. Goddard III, Nature 285 (1980) 311.
[34] A.K. Rappé and W.A. Goddard III, J. Am. Chem. Soc. 102 (1980) 5114.
[35] A.K. Rappé and W.A. Goddard III, J. Am. Chem. Soc. 104 (1982) 448.
[36] A.K. Rappé and W.A. Goddard III, J. Am. Chem. Soc. 104 (1982) 3287.